Modeling Heterogeneous Objects in CAD

Xiao J. Wu[1], Wei J. Liu[2] and Michael Y. Wang[3]

[1]Harbin Institute of Technology Shenzhen Graduate School, wuxj@hitsz.edu.cn
[2]Shenyang Institute of Automation, wjliu@sia.cn
[3]The Chinese University of Hong Kong, yuwang@mae.cuhk.edu.hk

ABSTRACT

A heterogeneous object (HO) modeling system independent of any commercial CAD software packages is introduced in this paper. Through this system, CAD models can be converted into 2D slices with heterogeneous material information for the fabrication of rapid prototyping technique. In this framework, volumetric dataset (VD) is employed to represent the material variations, which offers flexible manipulability to HO representation, while geometry model is used to describe the shape of an object, which can guarantee the accuracy of final HO slices. Two schemes are used to evaluate the composition variations in this system. Ray casting is utilized to render the HO volumetric dataset with the property of transparency.

Keywords: Heterogeneous object modeling, CAD system, Rapid prototyping, Volume Graphics

1. INTRODUCTION

Modeling and manufacturing of heterogeneous object (HO) has been paid much attentions recently as the advent of rapid prototyping manufacturing technology, which makes it possible to fabricate the object with material variations. A heterogeneous object is referred to a solid component consisting of two or more material primitives distributed continuously or discontinuously. As the continuous variation of material composition produces gradient in material properties, they are often known as functionally gradient materials (FGM), shown in Fig. 1(a). For example, a component contains two compositions, metal and heat resistance material (such as ceramic); the material distribution is illustrated in (b). From the figure we can see that metal increases its percentage gradually from one side to another (the red line), while the heat resistance material linearly reduces its fraction (the green line), which can avoid the stress concentration because of the thermal stress relaxation in transition of two materials, shown in (c). A discontinuous change in material composition generates distinct regions of material in the solid, which is usually called multi-material object (MMO) such as composite materials, as demonstrated in Fig. 2 [1]. MMO has been extensively used in industry or other fields for a long time; however, FGM has shown tremendous potential in many fields, such as aeronautics and astronautics, biomedical engineering, and nano-technology, etc.

In order to take full advantages of the greatest potential of heterogeneous objects, one must have matching capabilities for their computer modeling, analysis and design optimization. The primary focus of the recent research and development in these fields are on the computer representation schemes for heterogeneous objects, by extending the mathematical models and computer data structures of the modern solid modeling techniques to include discrete material regions of interfacial boundaries and heterogeneous properties.
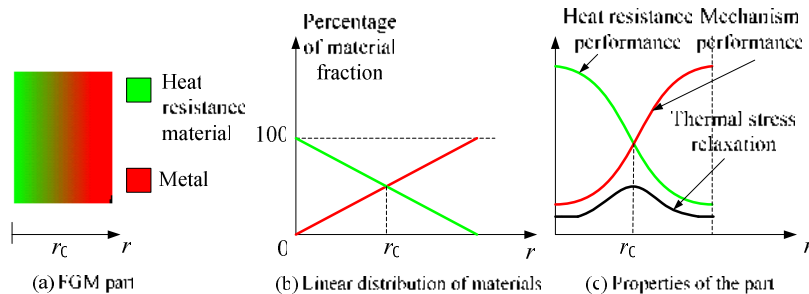

Fig. 1: Model of Functionally Gradient Materials.

Fig. 2: A multilaterals blade [1]

As a matter of fact, rapid prototyping can offer a possibility to fabricate the component with material variations because of the layer by layer and material additive characteristic of rapid prototyping manufacturing. Shape deposition manufacturing (SDM) of Carnegie Mellon University and Stanford University, laser engineered net shaping (LENS) of Sandia National Laboratory (SNL) has produced FGM parts with variety of metallic powders. With 3D printing, Massachusetts Institute of Technology (MIT) has created fine ceramic FGM components. Just as the color jet/laser printer can produce colorful pictures by using halftone technique in 2D, the heterogeneous object can also be fabricated by a 3D printer which is regarded as the most suitable means to create HO.

Approaches of modeling and representing a heterogeneous object have been extensively studied in computer and manufacturing community. Kumar and Dutta proposed an approach to model multi-material objects based on *R-m* sets and *R-m* classes primarily for application in layered manufacturing. Boolean operators to facilitate the modeling procedure were defined [2]. Jackson et al. proposed a local composition control (LCC) approach to represent heterogeneous object in which a mesh model was divided into tetrahedrons and different material compositions were evaluated on the nodes of the tetrahedrons by using Bernstein polynomials [3,4]. Chiu [5] developed a material tree structure to store different compositions of an object. The material tree was then added to a data file to construct a modified format suitable for RP manufacturing. Marsan and Dutta presented a method to model material properties in the form of tensor product surfaces within the framework of heterogeneous solid modeling [6].

Siu and Tan developed a scheme named 'source-based' method to distribute material primitives, which could vary any materials within an object [7]. The feature-based modeling scheme was extended to heterogeneous object representation through boundary conditions of a virtual diffusion problem in the solid, and then designers could use it to control the material distribution [8]. Liu et al. extended their work in [4] by taking parameterized functions in terms of distance(s) and functions using Laplace equation to blend smoothly various boundary conditions, through which designers could edit geometry and composition simultaneously [9]. Kou and Tan suggested a hierarchical representation for heterogeneous object modeling by using B-rep to represent geometry and a heterogeneous feature tree to express the material distributions [10]. Samanta et al. proposed an optimization problem is then constructed based on the object's functional requirements to calculate the optimum material variation. Variant models are easily generated by changing the geometric and material features using the constraints between them [11]. Chow and Tan was suggested a methodology and mathematical study on heuristic searching of optimal grid configuration to redesign heterogeneous continuous-attributed objects. The varying attributes of these objects are mapped into homogeneous attributes on finite spatial enumeration grids for attribute discretization [12]. Kou and Tan presented the data structures and algorithms for virtual prototyping of heterogeneous objects. Voxels are subsequently created and maintained in a dynamic scan-line structure, layered-section structure and the virtual-object structure at runtime [13].

Various methods for designing and optimizing objects composed of multiple regions with continuously varying material properties have been developed. Wang, Y. and Wang, X. proposed a level-set based variational scheme [14]. Biswas et al. presented a mesh-free approach based on the generalized Taylor series expansion of a distance field to model and analyze a heterogeneous object to satisfy the prescribed material conditions on a finite collection of material features and global constraints [15].

However, almost all of the research interests are mainly focused on the computer representation of heterogeneous object, rather than a complete pipeline for rapid prototyping fabrication of heterogeneous object. Most of the proposed approaches were verified in commercial software packages [9, 7], such as Solidworks, Unigraphics, etc. In [10], a commercial CAD package independent system is developed to deal with the HO modeling, but not including the slicing procedure for RP manufacturing. Kou and Tan explored approaches of the virtual prototyping of heterogeneous objects with run-time-created voxel scan-lines [13]. In this paper, we address the modeling system of heterogeneous object and all the supported modules. The detailed description of each module can not be presented for the paper length.

This paper is organized as follows: Section 2 is a brief review of our HO modeling system. The main modules are introduced in section 3. In the 4th section, some examples are presented and conclusion is the final part.

2. SYSTEM REVIEW

The procedures of HO modeling can be divided into two categories, parallel and sequential, that is whether the geometry and the material evaluation are designed simultaneously or the shape is modeled first and then material composition. As almost all of the commercial CAD software packages can only create geometric models, it is reasonable to take the sequential process as heterogeneous object modeling strategy in our system. The geometric model of implicit, explicit, polygon, CSG can be employed to describe the shape of an object as long as it is converted to volumetric dataset. For simplicity, we only use mesh models to demonstrate the efficiency of our algorithm.

In realistic world, the interior of *every* object is defined homogeneously or heterogeneously, instead of a shell with zero thickness. With the fast advances in computer hardware, especially faster, larger and cheaper memories available, computer graphics are being transformed from surface based to volume based, just like the transition from vector graphics to raster graphics in the seventies [16]. One of the most outstanding features of volumetric dataset is its capability to represent the inner structures of an object such that measurable properties, such as material, color, density, and strength, can be associated to each voxel. Therefore, it is a perfect choice to utilize volumetric dataset to describe the internal properties or structures of a heterogeneous object. In fact, voxel-based models are exploited for part modeling, analysis and manufacturing [16].

In our HO modeling scheme we take volumetric dataset as a carrier of material primitives, while the shape of the object is described by the geometric model. So it is convenient to manipulate the dataset and implement the boolean operations (e.g. union, difference, intersection, etc.), and the volumetric model can be easily processed to generate 2D slices which are essential to manufacturing with rapid prototyping techniques. Our scheme is illustrated in Fig. 3. These geometric and material models are flexible and efficient to evaluate different compositions.

Our HO modeling system contains five crucial modules. They are preparation of primary data structure module, heterogeneous material evaluation module, HO volumetric dataset visualization module, slicing file generation with gradient material information and display and file I/O module respectively. The geometry computation library offers lots of subroutines to process geometry computation. Fig. 4 shows the user interface of the system. The main modules are described specifically in the following section.
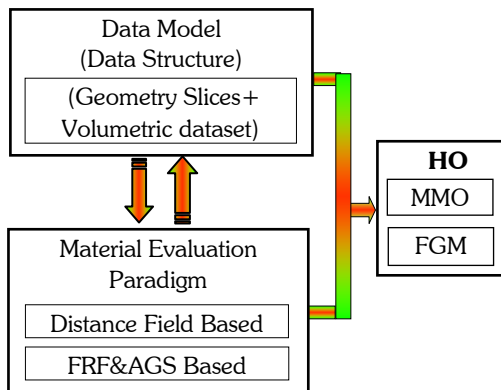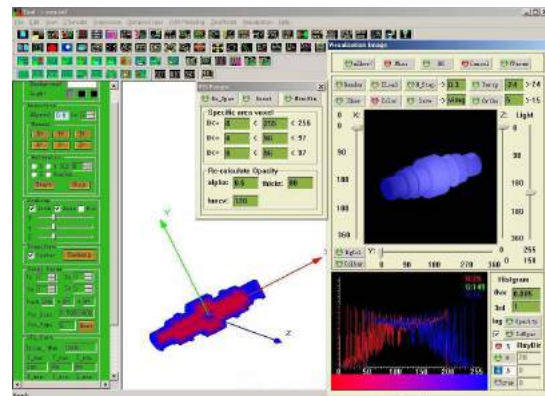

Fig. 3: Our scheme of HO Representation.

Fig. 4: User interface of HO representation.

3. SPECIFICATIONS OF SYSTEM MODULES

3.1 Primary Data Structures

This module includes two main sub-modules called data processing and voxelization. The data processing module mainly copes with the data structures for geometric model and the subdivision surfaces for improving the smoothness of meshes if a rough mesh model is input. In this case, a modified Loop scheme is used to subdivide the surfaces while maintaining the sharp features of the object.

Voxelization procedure converts a geometric model into volumetric dataset. As a matter of fact, volumetric dataset comes from a variety of fields, such as human organs scanned by Computer Tomography (CT) or Magnetic Resonance Imaging (MRI), the visual human project, scientific computation or simulation, computational fluid dynamics (CFD), meteorology, seismic exploration, etc. These datasets can be organized into Cartesian, regular, rectilinear, structured, unstructured and hybrid data format. In the past decade, a lot of methods on voxelization have been developed [18,19,20]. Most of the voxelization methods are an extension of the classical scanning conversion algorithm from 2D to 3D. In our HO representation, we develop a voxelization algorithm to convert geometric models into volume dataset based on [21]. For simplicity, we only utilize polygonal meshes (triangular meshes) to describe the voxelization algorithm, but all geometric models can be voxelized, such as CSG model, freeform surfaces, implicit or explicit surfaces [19, 21]. The algorithm is described briefly as follows.

Let S be a plane in 3D space, *G* and *H* be two planes parallel to *S* and locate opposite sides of *S* shown in Fig. 5. Their functions are expressed as equations (1) and (2).

$$Ax + By + Cz + D = 0 \qquad (1)$$

$$Ax + By + Cz + D \pm t = 0 \tag{2}$$

If plane S would be voxelized, just let the distances from the points between plane G and H satisfy equation (3)

$$-t \leq Ax + By + Cz + D \leq t \tag{3}$$

where t is defined as $t = t_6 = (L/2)\cos\beta$ if S is 6-adjacent voxel plane, and $t = t_{26} = K\cos\alpha = (L/2)\sqrt{3}\cos\alpha$, if S is 26-adjacent voxel plane. The definition of α, β, L, K and N are shown in Fig. 7. We use t_6 and t_{26} to replace t in function (3), then two theorems can be induced.

Theorem 1: Plane S is defined by A, B, C and D, the set $\tilde{S} = \{(x, y, z) \mid -t_6 \leq Ax + By + Cz + D \leq t_6\}$ defines a 6-adjacent voxel representation of S.

Theorem 2: Plane S is defined by A, B, C and D, the set $\tilde{S} = \{(x, y, z) \mid -t_{26} \leq Ax + By + Cz + D \leq t_{26}\}$ defines a 26-adjacent voxel representation of S.

Theorem1 and 2 are suitable for the voxelization of an indefinite plane [21]. In practice, the primitives, such as vertices, edges and faces, should be processed respectively for acceleration calculation. The sets of $\tilde{S}_v, \tilde{S}_e$ and $\tilde{S}_b$ represent the voxel sets of vertexes, edges and facets respectively. An object's voxel representation can be obtained from $\tilde{S} = \tilde{S}_v \cup \tilde{S}_e \cup \tilde{S}_b$. Taking a triangular facet as an example, say S, for each vertex of S we construct a sphere whose center is the vertex and the radius is R_c defined as $R_c = L/2$ when 6-adjacent and $R_c = (\sqrt{3}/2)L$ when 26-adjacent, showed in Fig.8(a). All the voxels within the sphere belong to set $\tilde{S}_v$. Similarly, for each edge of S, a bounding cylinder of radius R_c and length L is defined, where L is the length of the corresponding edge, seeing fig. 8(b). All the voxels inside the cylinder belong to set $\tilde{S}_e$. Thirdly, a bounding triangular box opposite to S is constructed with two S's parallel planes G and H and three planes, say $E_i (i = 1, 2, 3)$, perpendicular to S, showed in fig. 6(c). The voxels belonging to the box represent the voxelization of the triangle S.

An object is voxelized into volumetric dataset with different resolutions illustrated in Fig. 7 where (a) is a surface model, (b), (c) and (d) are the corresponding volumetric datasets. The resolutions are (64,64,45), (128,128,89) and (256,256,176) respectively. From (b), (c) and (d) we can see that the volumetric dataset are more approximate the surface based model with the increase of resolution. The algorithm details please refer to literatures of [19, 21].
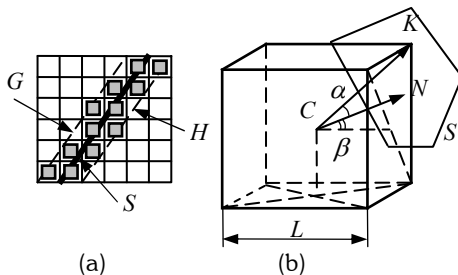

(a)   (b)
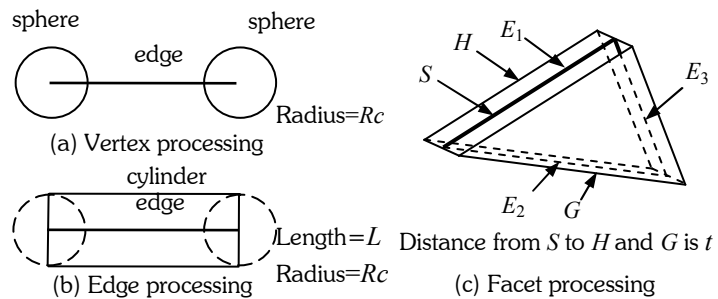
Fig. 5: (a) Rasterizing Line S, (b) The definition of α and β.

(a) Vertex processing

(b) Edge processing

(c) Facet processing

Fig. 6: The voxelization of vertex, edge and facet.

(a)Mesh model   (b) Resolution (64,64,45)   (c) Resolution (128,128,89)   (d) Resolution (256,236,176)
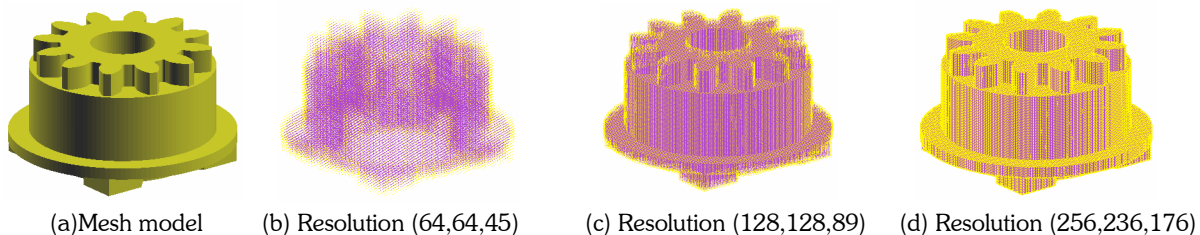
Fig. 7: A surface model and its volumetric dataset in different resolutions.

3.2 Evaluation of Heterogeneous Material

As described above, the core issue of heterogeneous object representation is designing a scheme to evaluate gradient or multi material within a CAD model according to the specification of users. In our system, we exploit the geometric model to describe the shape information. In terms of material information, we use the framework proposed by Kumar [2] to describe material composition in terms of material space which is a vector space and whose components are material primitives, for example, V^3 is a three dimensional material space constituted by three material primitives. The material space is notated as V^m with m material primitives.

Suppose Ω is a subspace of E^3 and $G_i (i = 1, 2, \cdots, k)$ are subsets of Ω. G_i satisfies the requirements (4)

$$\begin{cases} (G_1, G_2, \cdots, G_k) \in \Omega \\ G_1 \cap G_2 \cap \cdots \cap G_k = \varnothing \\ G_1 \cup G_2 \cup \cdots \cup G_k = \Omega \end{cases} \tag{4}$$

Defining space B is a subspace of V^m which is a material space with dimensions of m. Let $B_i (i = 1, 2, \cdots, k)$ are subspace of B, which is defined as a mapping of G_i in V^m. B_i should meet the requirements (5).

$$\begin{cases} (B_1, B_2, \cdots, B_k) \in B \\ B_1 \cap B_2 \cap \cdots \cap B_k = \varnothing \\ B_1 \cup B_2 \cup \cdots \cup B_k = B \end{cases} \tag{5}$$

A point in a heterogeneous object can be described as

$$P_v = \{(P_e, P_m) \mid P_e \in \Omega, P_m \in B\} \tag{6}$$

Then we can represent a heterogeneous object as following

$$P_{MMO} = \{(\boldsymbol{P}_{ei}, \boldsymbol{P}_{mi}) \mid \boldsymbol{P}_{ei} \in G_i, \boldsymbol{P}_{mi} \in B_i, \boldsymbol{P}_{mi} = \boldsymbol{C}; i = 1, 2, \cdots, N; j = 1, 2, \cdots, m\} \tag{7}$$

$$P_{FGM} = \{(\boldsymbol{P}_{ei}, \boldsymbol{P}_{mi}) \mid \boldsymbol{P}_{ei} \in G_i, \boldsymbol{P}_{mi} \in B_i, \boldsymbol{P}_{mi} = \nabla f \mid_{P_{mi}}; i = 1, 2, \cdots, N\} \tag{8}$$

where $\boldsymbol{C}$ is a constant material vector in a single B_i, and $\nabla f \mid_{P_{mi}}$ is the gradient determined by material distribution function, and N is the number of sampled points inside an object, namely object voxels.

To unify the MMO and FGM into a framework, we divide the object into several areas according to the distance field, notated as G_i whose mapping in material space is B_i. Currently, for a single material feature, only three subdivisions can be defined, denoted as $G_{-eff}, G_{eff}, G_{+eff}$, and the mapping to the material space is $B_{-eff}, B_{eff}, B_{+eff}$. These three subdivisions are defined as

- Negative Constant Material Range (NCMR): $G_{-eff} = \{\boldsymbol{P}_{ei} \mid \boldsymbol{P}_{ei} \in \Omega \,\&\, 0 \le d < \mathrm{d}_{-eff}\}$ (9)

- Material Gradient Range (MGR) G_{eff}: $G_{eff} = \{\boldsymbol{P}_{ei} \mid \boldsymbol{P}_{ei} \in \Omega \,\&\, \mathrm{d}_{-eff} \le d \le \mathrm{d}_{eff} + \mathrm{d}_{-eff}\}$ (10)

- Positive Constant Material Range (PCMR) G_{+eff}: $G_{+eff} = \{\boldsymbol{P}_{ei} \mid \boldsymbol{P}_{ei} \in \Omega \,\&\, d > \mathrm{d}_{-eff} + \mathrm{d}_{eff}\}$ (11)

where d is distance(s) from selected feature(s).

Generally, a material distribution function is needed to determine the material variation within an object, which comes from material designer or expert system of material design. This function takes the distance from inner object point to the selected feature(s) as arguments $0 \le f(x) \le 1$, and it must be satisfy the requirements of $0 \le f(x) \le 1$ in the material gradient range due to the summation of all the material primitives equal to 1. At the moment, $f(x)$ is single variable function to control the composition variation; any analytical, segmental, linear or nonlinear functions can be taken as material distribution function.

3.2.1 Distance Function Based Material Evaluation Paradigm

Let vector array $\boldsymbol{M}$ store the variations of materials, and each component of $\boldsymbol{M}$, say $\overline{\boldsymbol{m}}_j$, is a vector in size of m, the dimension of material space. $\boldsymbol{P}_{mi}$ is a point in material space, and $\boldsymbol{P}_{mi}$ is defined by $\boldsymbol{P}_{mi} = \{\overline{\boldsymbol{m}}_j \mid j = 1, 2, \cdots, m\}$, and $\overline{\boldsymbol{m}}_j$ should meet the following requirement.

$$\sum_{j=1}^{m} \bar{\boldsymbol{m}}_j = 1 \tag{12}$$

At present, only three material primitives can be evaluated by distance field based approach. The value of $\boldsymbol{P}_{mi}$ in MGR is defined by the following formula

$$\boldsymbol{P}_{mi} = \begin{pmatrix} [f(d - \mathrm{d}_{-\mathrm{eff}})] \\ [1 - (f(d - \mathrm{d}_{-\mathrm{eff}}) + C)] \\ C \end{pmatrix}, i = 1, 2, \cdots, N \tag{13}$$

where C is an invariable representing a constant material composition in the whole object. In this case, the composition function should be confined to $0 \le f(d) \le (1 - C)$. That the independent variable of $f(x)$ is $(d - \mathrm{d}_{-\mathrm{eff}})$ rather than d is because distance d is computed from reference feature(s), the material function $f(x)$ meets the condition of $0 \le f(x) \le 1$ in interval $[0, \mathrm{d}_0]$.

Defining $\boldsymbol{M}_s$ and $\boldsymbol{M}_e$ are the material vectors in the beginning and the end of material gradient range, which can be offered by designers, but it can not guarantee the continuity from NCMR to MGR and from MGR to PCMR. We can use the following equation to compute $\boldsymbol{M}_s$ and $\boldsymbol{M}_e$ to ensure the continuity.

$$\boldsymbol{M}_s = \begin{pmatrix} [f(\mathrm{d}_{-\mathrm{eff}})] \\ [1 - (f(\mathrm{d}_{-\mathrm{eff}}) + C)] \\ C \end{pmatrix} \text{ and } \boldsymbol{M}_e = \begin{pmatrix} [f(\mathrm{d}_{-\mathrm{eff}})] \\ [1 - (f(\mathrm{d}_{-\mathrm{eff}} + \mathrm{d}_{\mathrm{eff}}) + C)] \\ C \end{pmatrix} \tag{14}$$

As the above analysis, the material distribution in B_{-eff} can be defined as

$$G_{B-eff} = \{\boldsymbol{P}_{mi} \mid \boldsymbol{P}_{mi} \in B_{-eff} \,\&\, \boldsymbol{P}_{mi} \in \boldsymbol{M}_s\} \tag{15}$$

The material distribution in B_{eff} is defined as: $\quad G_{Beff} = \{\boldsymbol{P}_{mi} \mid \boldsymbol{P}_{mi} \in B_{eff}\} \tag{16}$

The material distribution in B_{+eff} is defined as: $\quad G_{B+eff} = \{\boldsymbol{P}_{mi} \mid \boldsymbol{P}_{mi} \in B_{+eff} \,\&\, \boldsymbol{P}_{mi} \in \boldsymbol{M}_e\} \tag{17}$

Thus, a HO model can be defined as: $\quad G = ((G_{-eff}, G_{B-eff}), (G_{eff}, G_{Beff}), (G_{+eff}, G_{B+eff})) \tag{18}$

From equation (10) we can see if MGR is vanish, HO is MMO, otherwise HO is FGM.

3.2.2 FRF&AGS-based Material Evaluation Paradigm

From the above subsection, we can see that Distance Field based method can only evaluate three compositions and two materials variations. It is inflexible and undesirable. Siu and Tan [7] proposed the 'source-based' scheme to represent any kind of material primitives according to the material feature. We modify this approach into our framework to overcome the drawback of distance field based method. As the computational expense is tremendous when taking a curve surface or model's contour as a feature, it is sensible to fix the feature unmovable when the material grading source is modified. The unmovable feature(s) are called fixed reference feature(s) (FRF), and the movable grading source is called active gradient source (AGS). By using this scheme, the 'source-based' approach can be effectively used in our HO representation framework.

A material vector of 'source-based' scheme in material gradient range can be modified as the equation (19)

$$\boldsymbol{P}_{mi} = \begin{bmatrix} \boldsymbol{m}_1 \\ \boldsymbol{m}_2 \\ \vdots \\ \boldsymbol{m}_m \end{bmatrix} = f(d - \mathrm{d}_{-\mathrm{eff}}) \times \begin{bmatrix} m_{e1} - m_{s1} \\ m_{e2} - m_{s2} \\ \vdots \\ m_{ej} - m_{sj} \end{bmatrix} + \begin{bmatrix} m_{s1} \\ m_{s2} \\ \vdots \\ m_{sj} \end{bmatrix}, \begin{cases} m_{sj} \in \boldsymbol{M}_s \\ m_{ej} \in \boldsymbol{M}_e \\ 0 \le f(d - \mathrm{d}_{-\mathrm{eff}}) \le 1 \end{cases}, \tag{19}$$

where $\boldsymbol{M}_s$ and $\boldsymbol{M}_e$ are the material vectors in start and end point of composition variations. Above equation is simplified as

$$\boldsymbol{P}_{mi} = f(d - \mathrm{d}_{-\mathrm{eff}})\boldsymbol{S}_m + \boldsymbol{M}_s, \tag{20}$$

where $\boldsymbol{S}_m = \boldsymbol{M}_e - \boldsymbol{M}_s$.

Similar with the distance field based method, the geometric and the material space are divided into three areas respectively, denoted as G_{-eff}, G_{eff} and G_{+eff} and B_{-eff}, B_{eff} and B_{+eff}. Also using G_{B-eff}, G_{Beff} and G_{B+eff} to denote the composition constitution in material space, FRF&AGS base representation scheme can be also expressed by formula (18). But in this case, $f(d)$ must be equal to zero, that is $f(d)=0$, in B_{-eff}, and $f(d)=1$ in B_{+eff}. With respect to just one material feature and one grading source, the composition is evaluated as follows

$$G_{B-eff} = \{\boldsymbol{P}_{mi} \mid \boldsymbol{P}_{ei} \in G_{-eff} \ \& \ \boldsymbol{P}_{mi} \in B_{-eff} \ \& \ f(d)=0\},$$ (21)

$$G_{Beff} = \{\boldsymbol{P}_{mi} \mid \boldsymbol{P}_{ei} \in G_{eff} \ \& \ \boldsymbol{P}_{mi} \in B_{eff}\},$$ (22)

$$G_{B+eff} = \{\boldsymbol{P}_{mi} \mid \boldsymbol{P}_{ei} \in G_{+eff} \ \& \ \boldsymbol{P}_{mi} \in B_{+eff} \ \& \ f(d)=1\}$$ (23)

From equation (19) we can see if d_{eff} equals to zero, heterogeneous object is FGM, otherwise it is MMO. Boolean operators facilitate the set operation in solid modeling. Likewise, we can also define heterogeneous representation Boolean operators. As we take volumetric dataset to represent the heterogeneous object, it is convenient to execute the Boolean operations.

3.3 HO Volumetric Dataset Visualization

As the volumetric dataset is a discrete representation of an object, the normal is lost in the voxelization procedure. Thus, the rendered image of HO is not realistic. However, direct volume rendering (DVR) in scientific visualization is a powerful tool to render volumetric datasets. DVR technique is mainly used in medical imaging, where volume data is available from CT, MRI or PET. DVR is an approximate simulation of the propagation of the light through a colored, semi-transparent gel where the color and opacity are functions of the scalar values in the volume dataset. The DVR algorithms fall into two categories, namely image based method and object based method, according to the ways of voxel projection. In our system we use a modified ray-casting algorithm to render volume dataset of heterogeneous object. Traditionally, volumetric dataset is projected onto an image plane by assigning a color and opacity to each voxel. For the HO volumetric dataset, the color information has been computed to represent the material properties. We use a modified ray-casting pipeline to render HO representation. Fig. 8 gives two rendered results from different volumetric datasets of heterogeneous object, from which we can see that the images reveal the realistic result of 3D object and the transparency by proper rendering parameters. At present, the average rendering time cost is almost ten seconds for a mediate dataset with image size of 256x256. The optimized real time rendering algorithm for volumetric dataset of heterogeneous object is one of our future research plans.
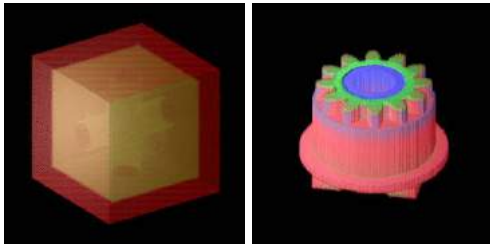

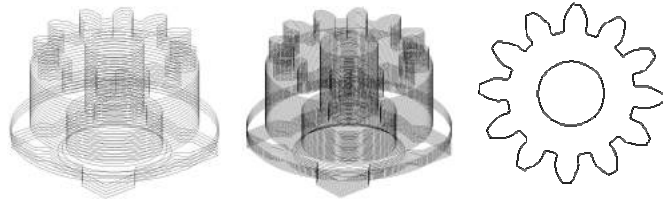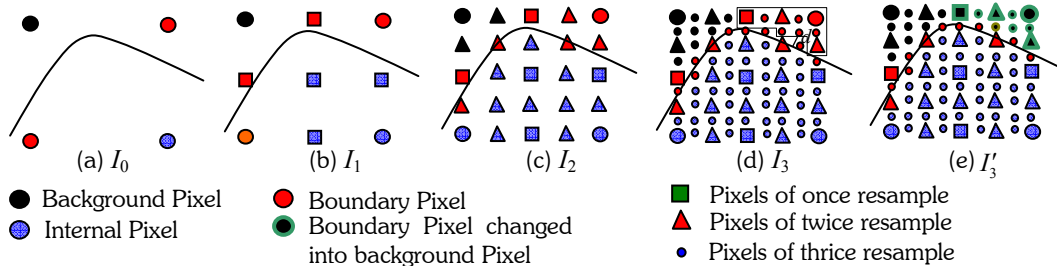Fig. 8: Ray-casting rendered images of HO.　　Fig. 9: Slices of object with different thickness.

Fig. 10: Material resample with geometric constraint in 2D.

3.4 Heterogeneous Material Slicing Generation

As described in the introduction, rapid prototyping technique offers a possibility to manufacture heterogeneous part. The accuracy and quality of the final part fabricated by rapid prototyping depends on the 2D geometric slices of a model. The slicing contours describe the boundaries of the object to be fabricated. The inner of the contours are filled in the way of hatching, also called path planning. However, this strategy is not suitable for the manufacturing of HO as it requires not only the geometric information but also the material variations. In our HO representation scheme, we utilize the slices of the geometric model and the layers of the material volumetric dataset to construct the 2D slices of heterogeneous object to guarantee the accuracy of the slicing contours, which is called material resample with geometric constraint (MRGC).

The geometry slicing algorithms are studied extensively in rapid prototyping community. There are mesh-based, direct, adaptive and hybrid slicing algorithms. In our framework, a mesh model slicing algorithm is developed based on directional weighted graph. Fig.9 shows a gear model sliced with different layer of thickness. The geometric contour is continuous in geometric space, which can be used to represent the shape of the object while the material information can be resampled to fill the contour. MRGC is divided into two steps; one is resampling along z axis, the direction of manufacturing, according to the thickness of geometric slices to meet the demands of fabrication. Another step is sampling each material layer on the geometric contour plane by interpolation method, shown in Fig.10. Fig.10 (a) is a curve segment and its rasterization. Figures (b) to (d) are three times resampling of the original image. In (d) we find that the pixels under the frame do not contribute to shape representation of the object. Thus these invalid pixels can be tagged as background pixels, seeing (e). In practice, whether a pixel is an invalid pixel can be determined by a threshold that is the distance from outer pixels on the boundary to the geometrical contours.
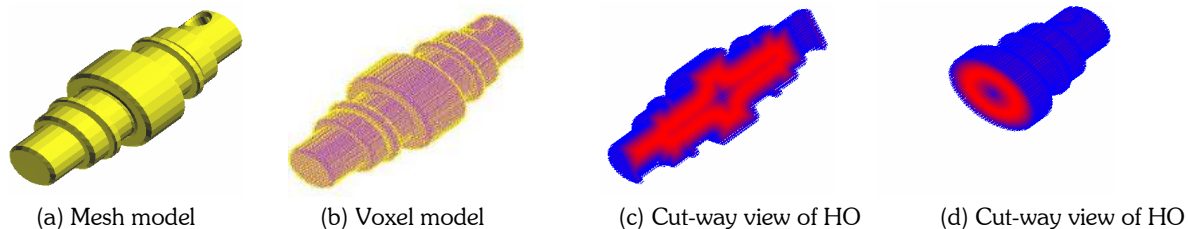

| (a) Mesh model | (b) Voxel model | (c) Cut-way view of HO | (d) Cut-way view of HO |

Fig. 11: HO representation of a shaft.

4. EXAMPLES

For paper length limitation, only a FRF&AGS example is presented. Fig.11 (a) is a shaft with dimension (150,55,55). It is volumetric representation is illustrated as (b) with resolution of (256,97,97). This component consists of three composition primitives. The contour of the model is chosen as reference feature to calculate distance map. The modeling parameters are as follows. m=3, d_{-eff}=0, d_{eff}=20.416 and d_{+eff}=0. A sinusoid function, $f(d) = \sin(0.1538d)$, is taken as material distribution function. The material vectors at the start and end point are $M_s = [0,0,1.0]$ and $M_e = [0,0.2,0.8]$. Equations (21), (22) and (23) are utilized to evaluate the compositions. The final results are presented in Fig.11 (c) and (d).

In Fig.12, we extract the slices of the HO along axis and radius, showed in (b) and (c). Figures (d) (e) and (f) (g) are the corresponding material spatial distribution on slices (b) and (c), from which we can see that the material is evaluated in accordance with material distribution function. Furthermore, the HO slices are sampled on three orthogonal lines through the center of the shaft, shown in (b) and (c) lines S_1, S_2 and S_3. The curve shown in Fig.13 (a) is the material distribution function (MDF) graph according to a given distance map Figs.13 (b) (c) and (d) show the material distribution (MD) on the sample lines, from which we can see that the results from our system is almost same as the theoretical model.

Fig.14 is an example of slicing strategy, where (a) is a layer of geometric slice contour and a voxel layer drawn on same image. Figure (b) is the image constructed from the voxel layer directly. The resolution is very low, and then this image is resampled four times. After the invalid pixels were abandoned, we obtained an image with high resolution and clear boundary exactly with the corresponding geometric contour, for clearness only three portions of the image are displayed in figures (c), (d) and (e). Figure (f) is an enlarged part of image (b) using simple interpolation scheme without geometry constraint, from which we can find that the edge of the image is very blurry. We can also use the geometric contours produced by direct slicing or adaptive slicing algorithm as constraints to reconstruct the HO slices.

In this case, the accuracy of HO slices is determined completely by the resample resolution. It is clear that we can theoretically construct accurate slices with heterogeneous information exactly as long as the resample resolution is high enough. However, it will increase the computational and storage cost. It is unnecessary to resample the material voxel layer to extremely high resolution. As long as the accuracy of the layers satisfies the manufacturing requirement, it should be stopped. The slices can be employed to produce the path planning using halftone or other methods.
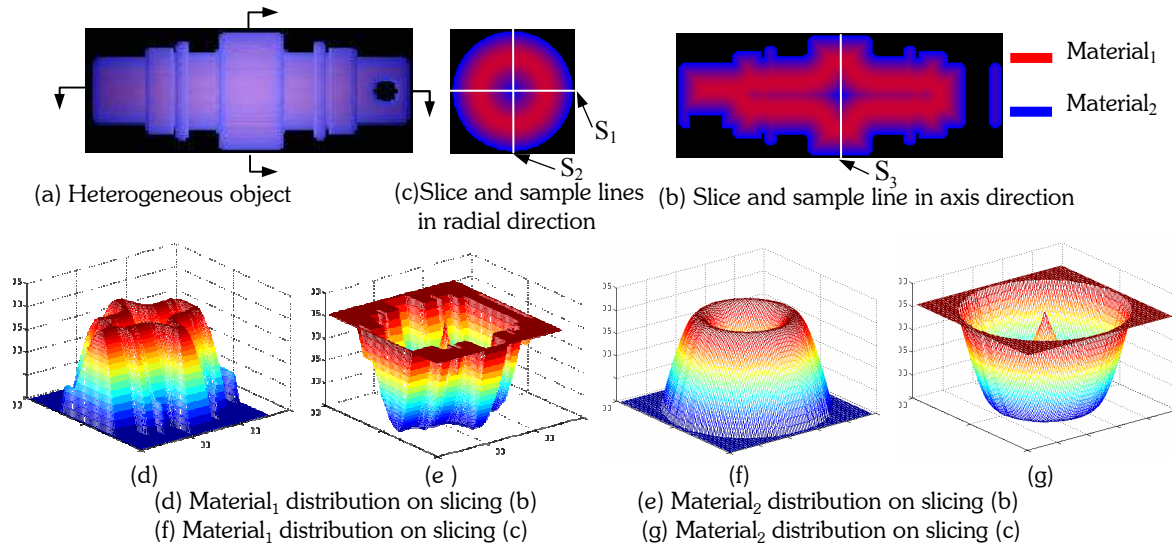

(a) Heterogeneous object

(c)Slice and sample lines in radial direction

(b) Slice and sample line in axis direction

(d) Material$_1$ distribution on slicing (b)
(e) Material$_2$ distribution on slicing (b)
(f) Material$_1$ distribution on slicing (c)
(g) Material$_2$ distribution on slicing (c)

Fig. 12: HO and material distribution on slices.
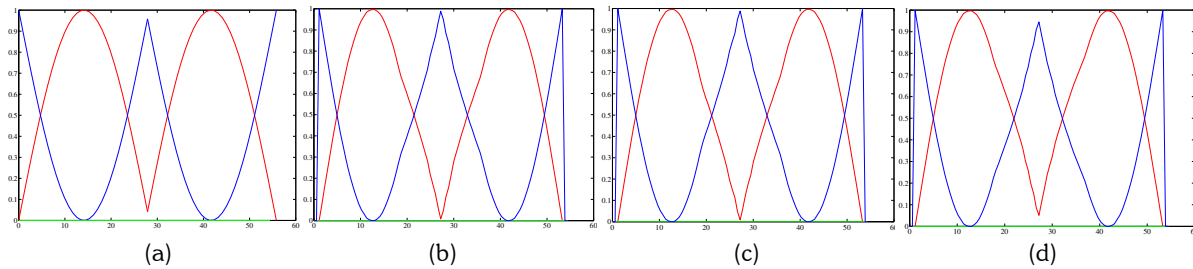

(a)   (b)   (c)   (d)

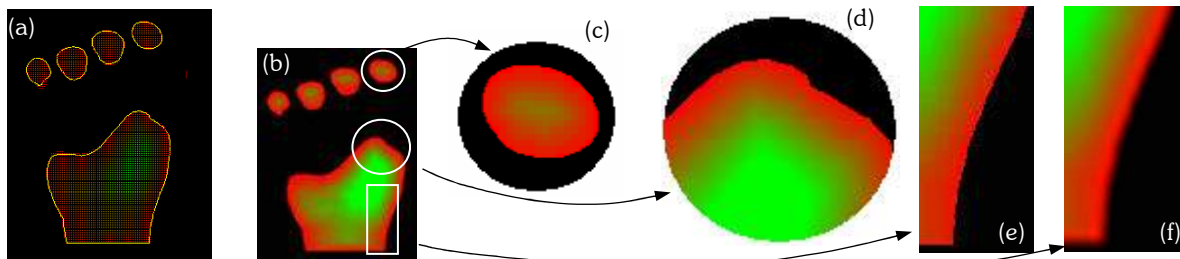Fig. 13: Material analysis on sample lines.

Fig. 14: An example of MRGC, (a) a layer of volume dataset and a geometrical contour, (b) a HO slice constructed from (a) directly, (c)-(d) are three parts of the enlarged image with clear boundaries.

5. CONCLUSIONS

In this paper we present a prototype system of heterogeneous object modeling independent of any commercial software packages. Each of modules of the system is introduced specifically. This system can offer a pipeline from CAD model to 2D slices with heterogeneous (composite and gradient) material. Our approach increases the flexibility of heterogeneous object modeling with the volumetric dataset structure but not lose the accuracy of HO slices under the constraint of geometric slicing contours. Moreover, slices of the heterogeneous object can be easily generated and the HO volumetric dataset can be visualized with ray casting method to show the specific material distribution within an object. Though mesh model is utilized to represent the geometry of an object in our system, other file format can be easily integrated into our system as the direct slicing algorithm can generate the slices which do not influence the representation of the material variations. The development of this system can facilitate the design, visualization and fabrication of heterogeneous object. Examples demonstrate the effectiveness of the heterogeneous object modeling system.

6. REFERENCES

[1]   www.zcorp.com
[2]   Kumar, V.; Dutta, D.: An approach to modeling & representation of heterogeneous objects, Journal of Mechanical Design, 1998, 120, 659-667.
[3]   Jackson, T. R.: Analysis of functionally graded material object representation methods, PhD thesis, Massachusetts Institute of Technology (MIT), Cambridge, MA, January 2000.
[4]   Liu, H. Y.: Algorithms for design and interrogation of functionally graded material solids, Master's thesis, Massachusetts Institute of Technology, Cambridge, MA, January 2000.
[5]   Chiu, W. K.; Tan, S. T.: Multiple material objects: from CAD representation to data format for rapid prototyping, Computer-Aided Design, 32, 2000, 707-717.
[6]   Marsan, A.; Dutta, D.: On the application of tensor product solids in heterogeneous solid modeling, Proceedings of 1998 ASME Design Engineering Conferences, Sep. 1998, Atlanta, Georgia, 1-9.
[7]   Siu, Y. K.; Tan, S. T.: 'Source-based' heterogeneous solid modeling, Computer-Aided Design, 34(1), 2002, 41-55.
[8]   Qian, X.; Dutta, D.; Feature-based design for heterogeneous objects, Computer-Aided Design, 36(12), 2004, 1263-1278.
[9]   Liu, H. Y.; Maekawa, T.; Patrikalakis, N. M.; Sachs, E. M.; Cho, W.: Methods for feature-based design of heterogeneous solids, Computer-Aided Design, 36, 2004, 1141-1159.
[10]   Kou, X. Y.; Tan, S. T.: A hierarchical representation for heterogeneous object modeling, Computer-Aided Design, 37(3), 2005, 307-319.
[11]   Samanta, K.; Koc, B.: Heterogeneous object design with material feature blending, Computer-Aided Design & Applications, 1(1-4), 2004, 429-437.
[12]   Chow, H. N.; Tan, S. T.; Sze, W. S.: Re-designing heterogeneous objects by attribute discretization, Computer-Aided Design & Applications, 2(1-4), 2005, 387-392.
[13]   Kou, X.Y.; Tan, S. T.: Data structure and algorithms for virtual prototyping of heterogeneous objects, Computer-Aided Design & Applications, 3(1-4), 2006, 59-67.
[14]   Wang, M. Y.; Wang, X. M.: A level-set based variational method for design and optimization of heterogeneous objects, Computer-Aided Design, 37(3), 2005, 321-337.
[15]   Biswas, A.; Shapiro, V.; Tsukanov, I.; Heterogeneous material modeling with distance fields, Computer Aided Geometric Design, 21(3), 2004, 215-242.
[16]   Kaufman, A.; Cohen, D.; Yagel, R.: Volume graphics, IEEE Computer, 26(7), 1993, 51-64.
[17]   Chandru, V.; Manohar, S.; Prakash, C. E.: Voxel-based modeling for layered manufacturing. IEEE Computer Graphics and Applications, 15(6), 1995, 42-47.
[18]   Kaufman, A.; and Shimony, E.: 3D scan conversion of polygons, Proceedings of EUROGRAPHICS'87 Conference, Amsterdam, The Netherlands, August 1987, 197-208.
[19]   Jones, M. W.; Satherley, R.: Voxelisation: modeling for volume graphics. In B. Girod, G. Greiner, H. Niemann, H. -P. Seidel (eds.), Vision, Modeling, and Visualization 2000, IOS Press, 319-326.
[20]   Kong, T. Y.; Rosenfeld, A.: Digital topology: introduction and survey, Computer Vision, Graphics, and Image Processing archive, 48(3), 1989, 357-393.
[21]   Huang, J.; Yagel, R.; Fillipov, V.; Kurzion, Y.: An accurate method to voxelize polygonal meshes, IEEE Volume Visualization'98, October, 1998, Chapel Hill, North Carolina, USA, 119-126.